Cell Reports, Volume *42*

Supplemental information

Adhesion analysis via a tumor vasculature-like microfluidic device identifies CD8$^+$ T cells with enhanced tumor homing to improve cell therapy

Camila P. Camargo, Abir K. Muhuri, Yunus Alapan, Lauren F. Sestito, Megha Khosla, Margaret P. Manspeaker, Aubrey S. Smith, Chrystal M. Paulos, and Susan N. Thomas

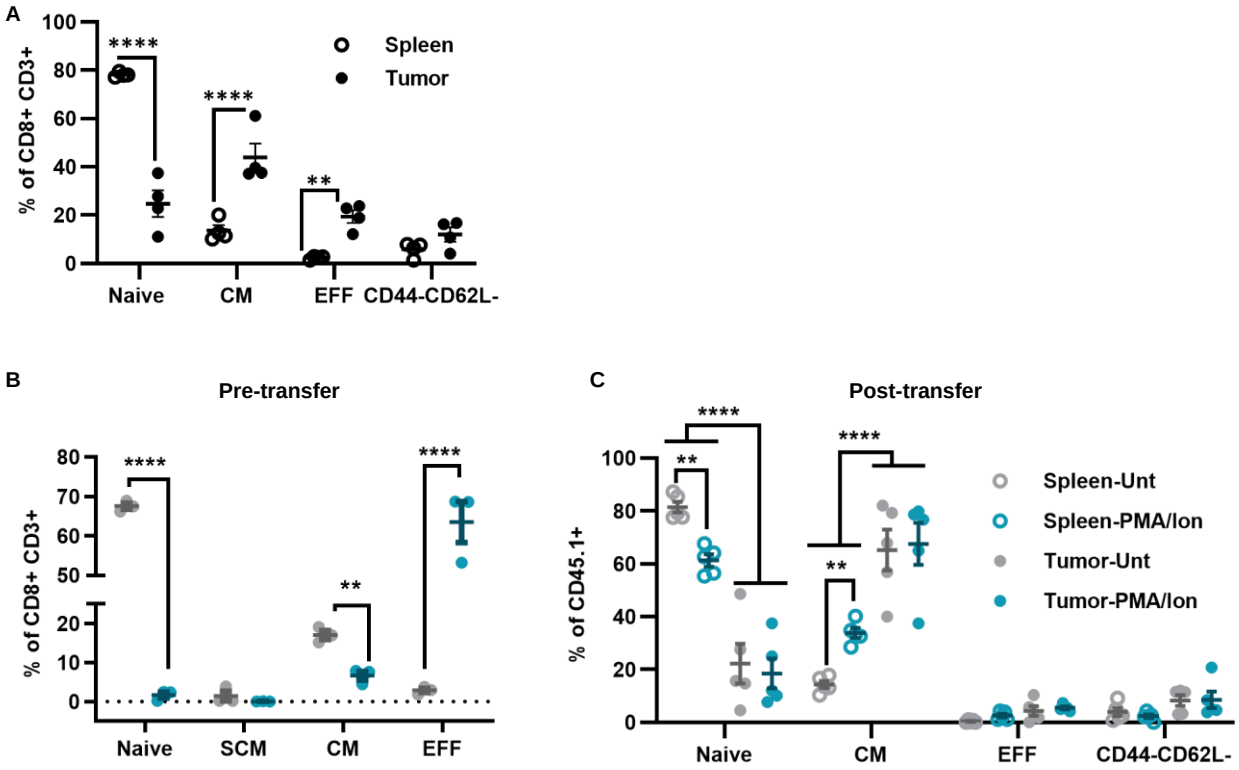

Supplemental Figure 1. CD8+ T-cells exhibiting more differentiated phenotypes are enriched within the TME compared to lymphoid tissues in day 7 B16F10 melanoma bearing mice. Related to Figure 1. A) Percent of endogenous CD8+ T-cells of various subtypes (Naïve, CD44-CD62L+SCA-1-; stem cell memory [SCM], CD44-CD62L+SCA-1+; central memory [CM], CD44+CD62L+; and effector cells [EFF], CD44+CD62L-) in the spleens or tumors of day 7 B16F10 tumor-bearing animals. B) Frequency of CD8+ T cell subtypes isolated from spleens and left untreated or treated with PMA/Ion prior to transfer. C) Percent of CD8+ T-cell subtype of CD45.1+ cells recovered from spleens and tumors of day 7 B16F10 melanoma bearing animals 16 h post transfer of 10^6 CD45.1+ CD8+ T cells. Points represent individual animals and data represent the mean ± s.e.m. Statistics performed by two-way ANOVA with Bonferroni's multiple comparisons test. **p<0.01, ****p<0.0001.

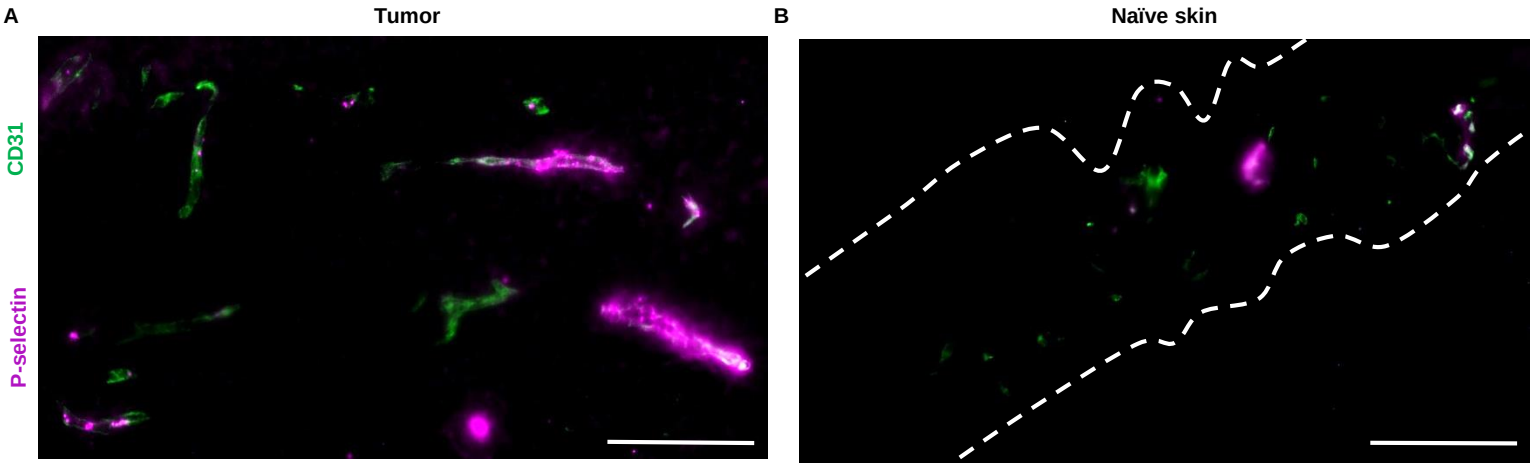

Supplemental Figure 2. Tumor vasculature exhibits more P-selectin expression compared to naïve skin. Related to Figure 1. Immunohistochemistry staining for P-selectin (red) and CD31 (green) in 8 µm thick sections of day 7 B16F10 tumors (A) formed in C57Bl/6 mice or naïve skin (B) from C57Bl/6 mice. Scale bar: 50 µm.

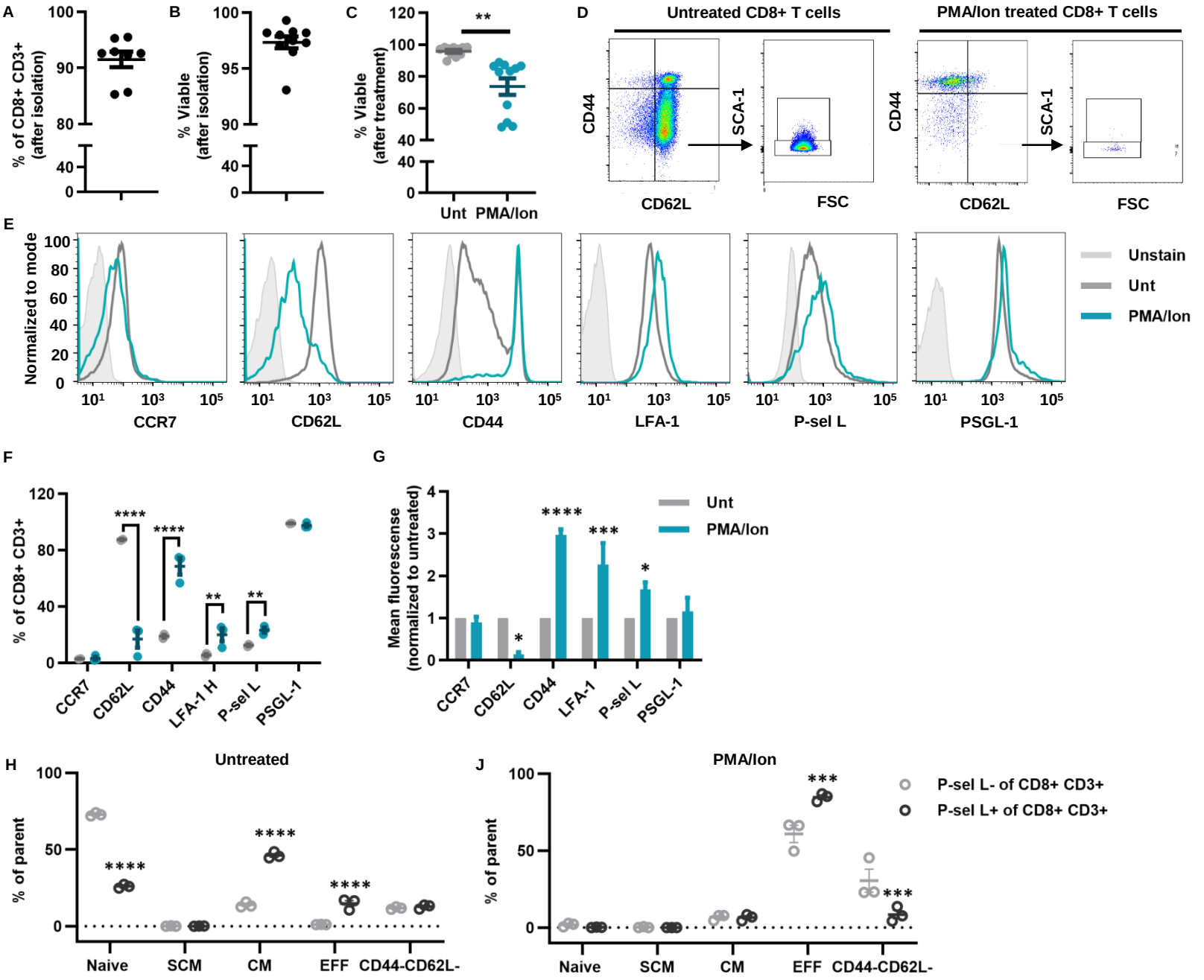

Supplemental Figure 3. Characterization of CD8+ T-cells prior to transfer. Related to Figure 1. Purity (A) and viability (B) of cells after CD8+ T-cell negative isolation from murine C57BL/6 spleens. C) Viability of CD8+ T cells after PMA/Ion treatment. Statistics analyzed by two-tailed parametric t-test. D) Representative flow cytometry plots of subtypes of CD8+ T-cells of untreated or PMA/Ion treated CD8+ T cells. Naïve, CD44-CD62L+SCA-1-; stem cell memory [SCM], CD44-CD62L+SCA-1+; CM, CD44+CD62L+; and EFF, CD44+CD62L-. E) Histograms of adhesion molecule expression by untreated or PMA/Ion treated CD8+ T-cells. Data from panel (E) represented as frequency of CD8+ T-cells (F) and normalized to untreated cell mean fluorescence (G). Frequency of various subtypes of CD8+ T-cells of P-selectin ligand +/- within CD8+ CD3+ untreated (H) and PMA/Ion populations (J). Points represent individual animals and data reflect the mean ± s.e.m. F-J, statistical comparisons were performed by two-way ANOVA with Bonferroni's multiple comparisons test. * p<0.05, **p<0.01,. *** p<0.001, ****p<0.0001.

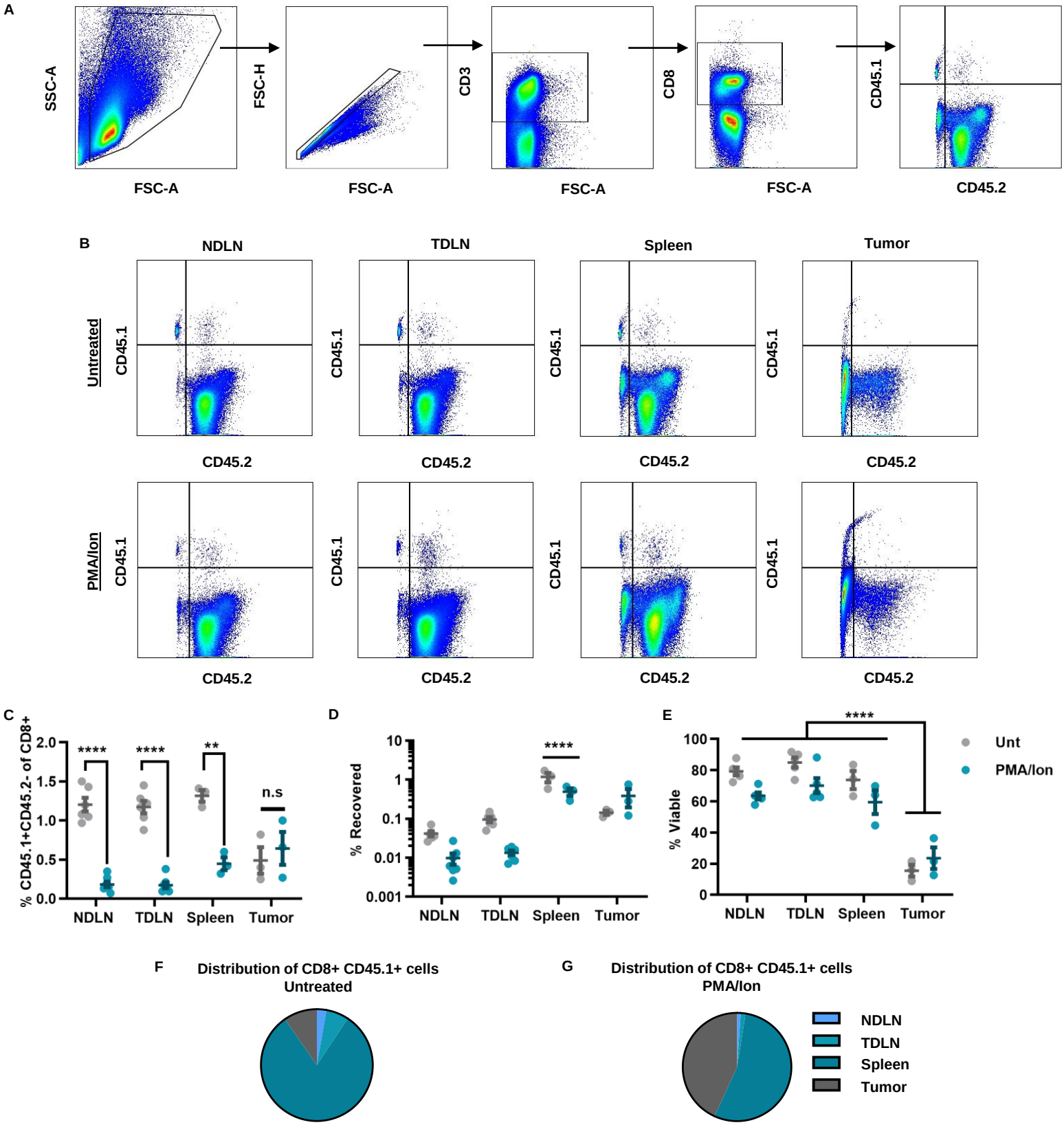

Supplemental Figure 4. Flow cytometry gating strategy and biodistribution analysis of untreated or PMA/Ion CD8+ T-cells adoptively transferred into B16F10 tumor bearing animals. Related to Figure 1. A) Flow cytometry gating strategy for donor CD45.1+ CD8+ T-cells adoptively transferred into recipient CD45.2+ animals bearing day 7 B16F10 melanomas. B) Representative flow cytometry scatter plots of adoptively transferred CD8+ T-cells (CD45.1+CD45.2-) recovered from various tissues 16h post transfer. C) Frequency of donor cells recovered of total CD8+ T-cells (donor and recipient) in each tissue. D) Frequency of recovered donor cells in each tissue of total adoptively transferred cells. E) Viability of trafficked CD8+ T-cells in each analyzed tissue. Distribution of untreated (F) and PMA/Ion (G) treated CD8+ T-cells recovered from each analyzed tissue. Points represent individual animals and data represent mean ± s.e.m. Statistics performed by two-way ANOVA with Bonferroni's multiple comparisons test. **p<0.01, ****p<0.0001.

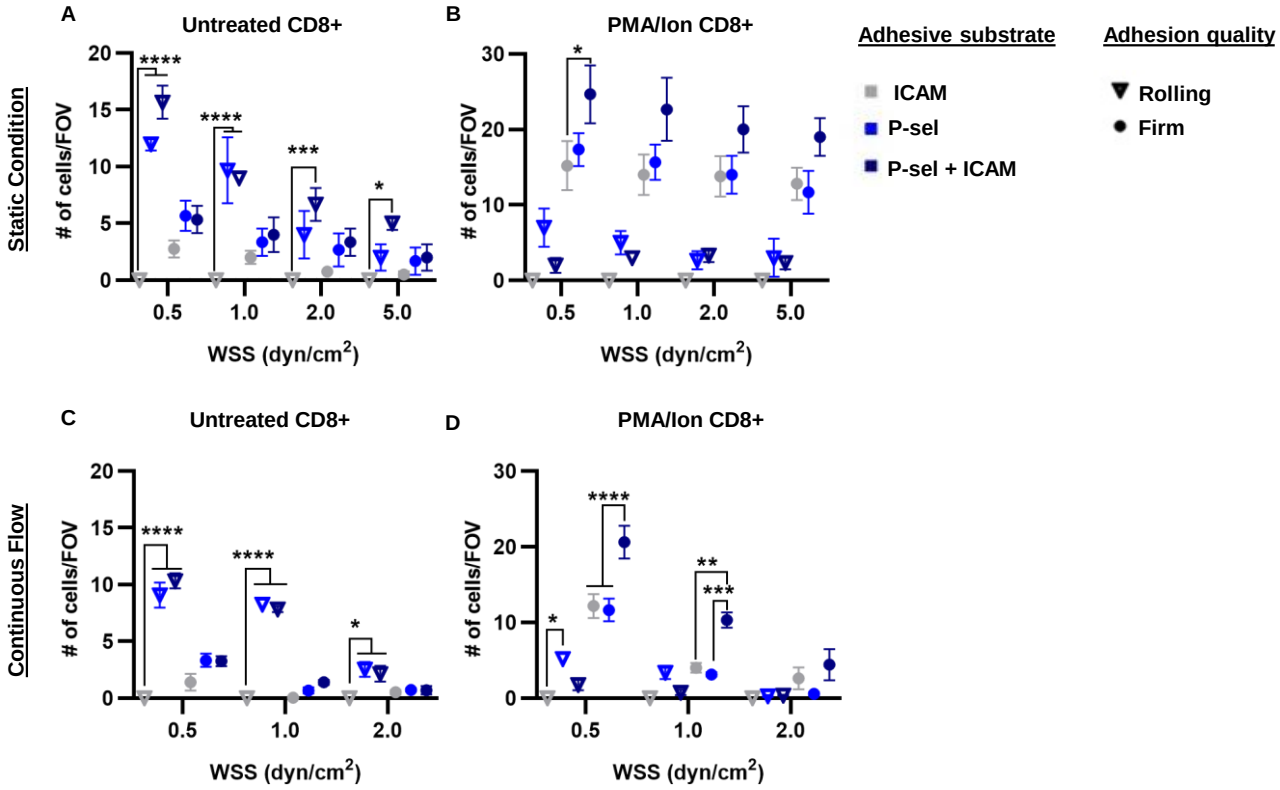

Supplemental Figure 5. Untreated and PMA/Ion activated CD8+ T-cells adhere to P-selectin, but only activated CD8+ T-cells adhere to ICAM. Related to Figure 2. Number untreated (A) or PMA/Ion treated (B) CD8+ T cells per field view interacting with an ICAM, P-selectin, or P-selectin + ICAM functionalized substrate under static conditions when deadhesion is initiated at the indicated levels of wall shear stress (WSS). Number of untreated (C) or PMA/Ion treated (D) CD8+ T cells per field view interacting with an ICAM, P-selectin, or P-selectin + ICAM functionalized substrate under continuous flow at the indicated levels of WSS at 0.5x10^6 cells/ml. Data represent mean ± s.e.m for three or more independently run experiments. Statistical comparisons performed by two-way ANOVA with Tukey's multiple comparisons test. * p<0.05, **p<0.01. *** p<0.001, ****p<0.0001.

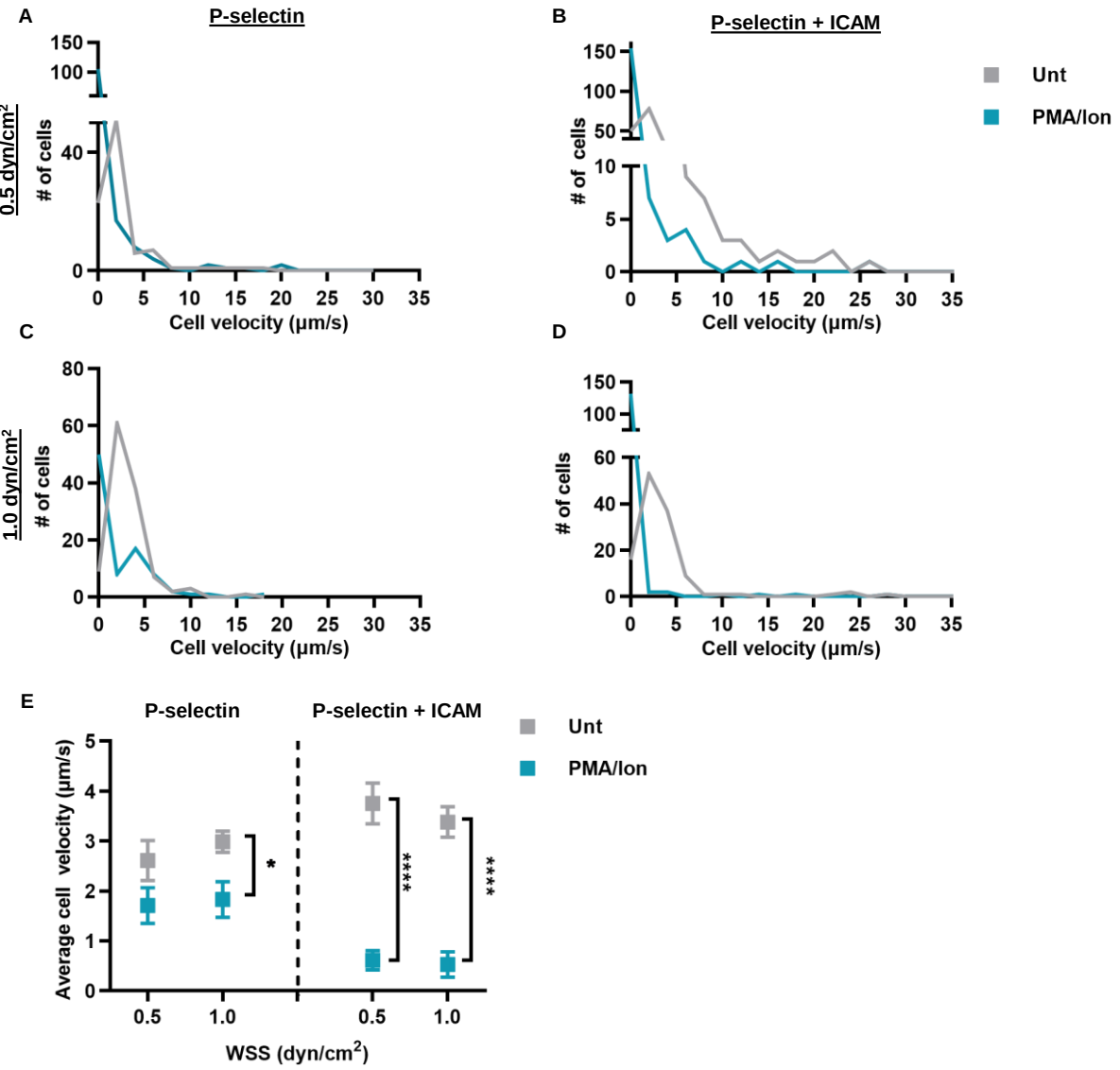

Supplemental Figure 6. PMA/Ion treated CD8+ T-cells exhibit lower velocities of rolling adhesion to P-selectin with or without ICAM compared to untreated CD8+ T cells. Related to Figure 2. A-D) Histograms of adhesion velocity of cells interacting with substrates functionalized with P-selectin alone or in combination with ICAM at varying WSS under conditions of continuous flow. E) Average velocities of interacting cells calculated from panels (A-D). Data represents mean ± s.e.m. for three independently run experiments. Statistical comparisons performed by two-way ANOVA with Dunnett's multiple comparisons test. * $p<0.05$, **** $p<0.0001$.

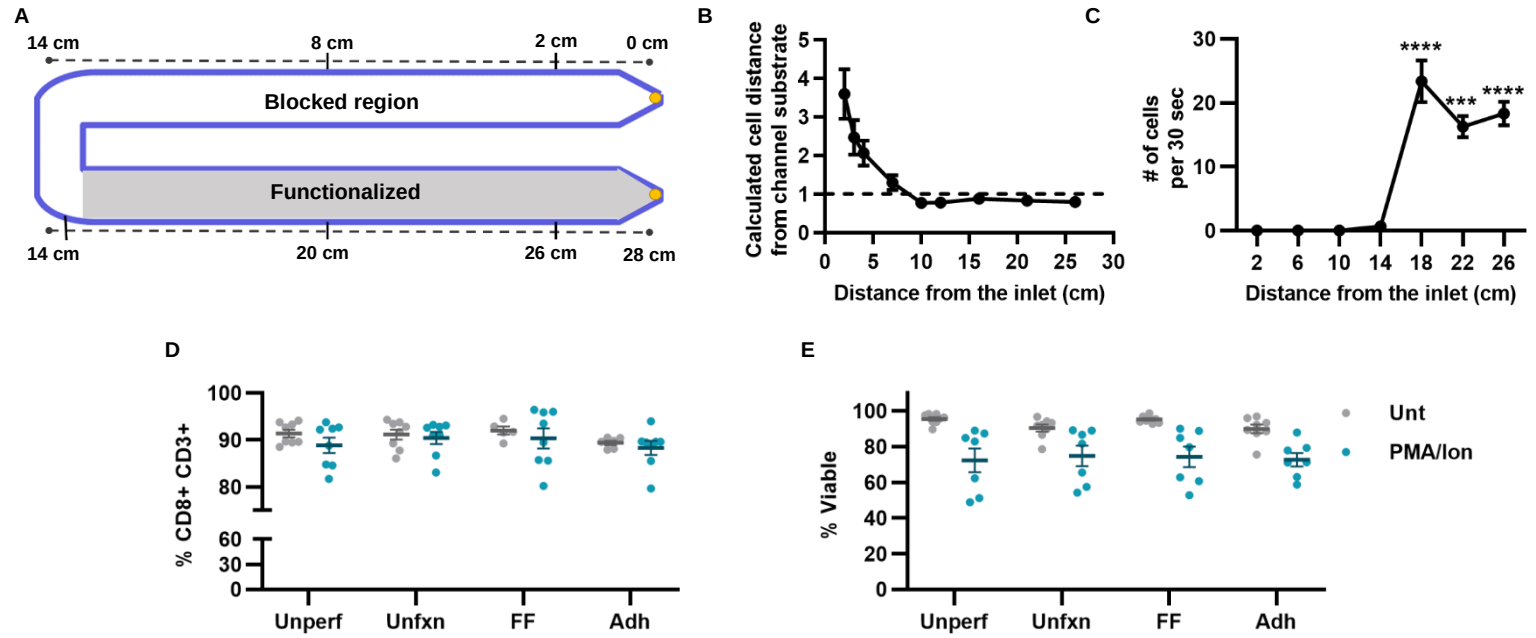

Supplemental Figure 7: Validation of engineered adhesion chromatography microfluidic system to investigate CD8+ T-cell adhesion under physiological levels of fluid flow *in vitro*. Related to Figure 3. A) Schematic outlining the top view of the channel of the adhesion chromatography microfluidic system. B) Distance of individual perfused CD8+ T-cells from the inferior substrate of an unfunctionalized channel calculated based on measured individual cell velocity and size. C) Number of interacting cells along the length of the channel during the sorting phase. Statistics for were performed by one-way ANOVA with Dunnett's multiple comparisons test Purity (D) and viability (E) of unperfused cells and cells perfused through either an unfunctionalized (Unfxn) channel or 25 ug/ml P-selectin functionalized fractionated into free flow (FF) and adherent (Adh) fractions at 0.5 dyn/cm^2. Statistics for D-E were performed by two-way ANOVA with Tukey's multiple comparison test. D-E, Each data point reflects results using splenocytes harvested from an individual animal. Data represents mean ± s.e.m. Results represent a minimum of three independently performed experiments.

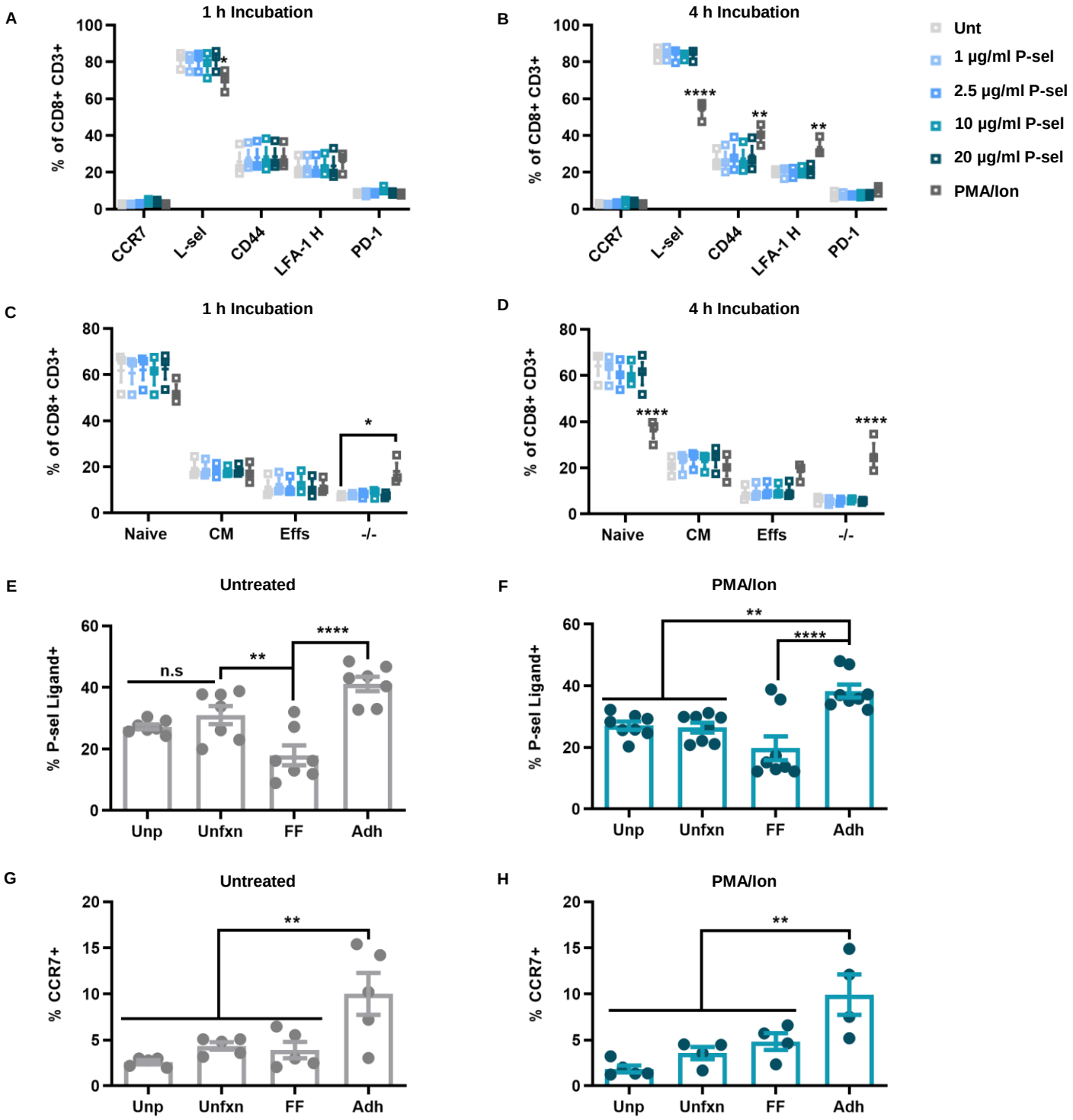

Supplemental Figure 8. Stimulation with P-selectin in solution or through a functionalized channel in flow does not activate CD8+ T-cells or increase their expression of CCR7. Related to Figure 3. Effects of CD8+ T-cell co-incubation with P-selectin chimera at varying concentrations for 1 (A, C) or 4 (B, D) hours on adhesion marker expression (A-B) and differentiation state (C-D). Mean ± s.e.m, p value from two-way ANOVA with Dunnett's multiple comparisons test. Percent P-selectin ligand+ (E-F) and CCR7+ (G-H) cells of untreated (E, G) or PMA/Ion pre-treated (F, H) CD8+ T-cells that were unperfused, perfused through an unfunctionalized (Unfxn) channel, or and perfused through a 25 ug/ml P-selectin functionalized channel at 0.5 dyn/cm^2 and sorted into FF and Adh fractions. Mean ± s.e.m, p value from one-way ANOVA with Tukey's multiple comparisons test; * p<0.05, **p<0.01, *** p<0.001, ****p<0.0001.

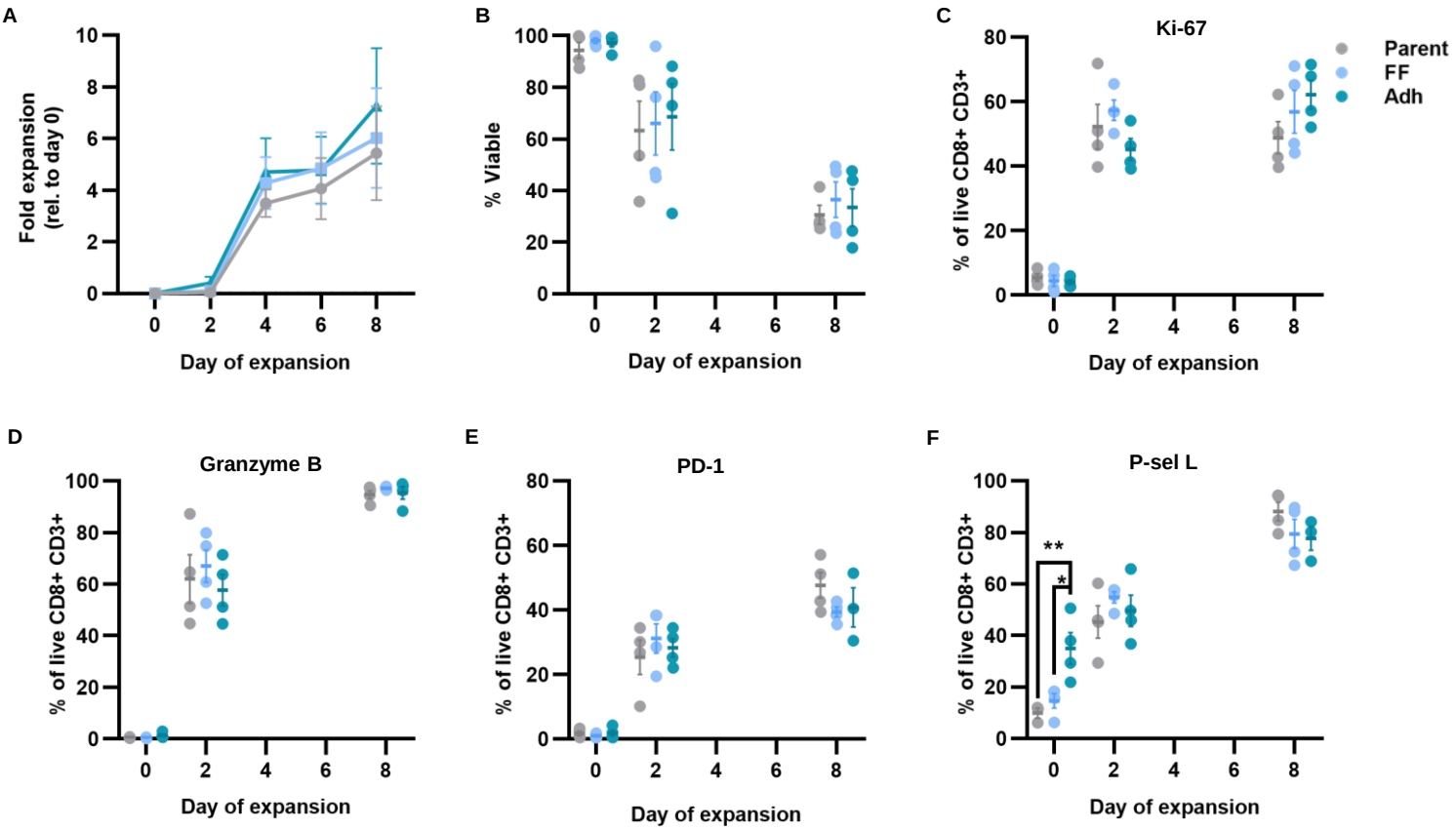

Supplemental Figure 9. Expansion of CD8+ T-cells enriched for adhesion to P-selectin in flow using adhesion chromatography microfluidic system. Related to Figure 3. A) Fold expansion of fractionated CD8+ T-cells cultured with Dynabeads with 100 UI/ml IL-2. B) Frequency of Ki-67+ of live CD8+ T cells throughout expansion. C) Viability of fractionated CD8+ T cells throughout expansion. Frequency of P-sel L (D), granzyme B (E), and PD-1 (F) of live CD8+ T-cells throughout expansion. Points represent an individual expansion. Data represents mean ± s.e.m. Results represent a minimum of three independently performed experiments. Statistical comparisons performed by two-way ANOVA with Dunnett's multiple comparisons test. * $p<0.05$, ** $p<0.01$.

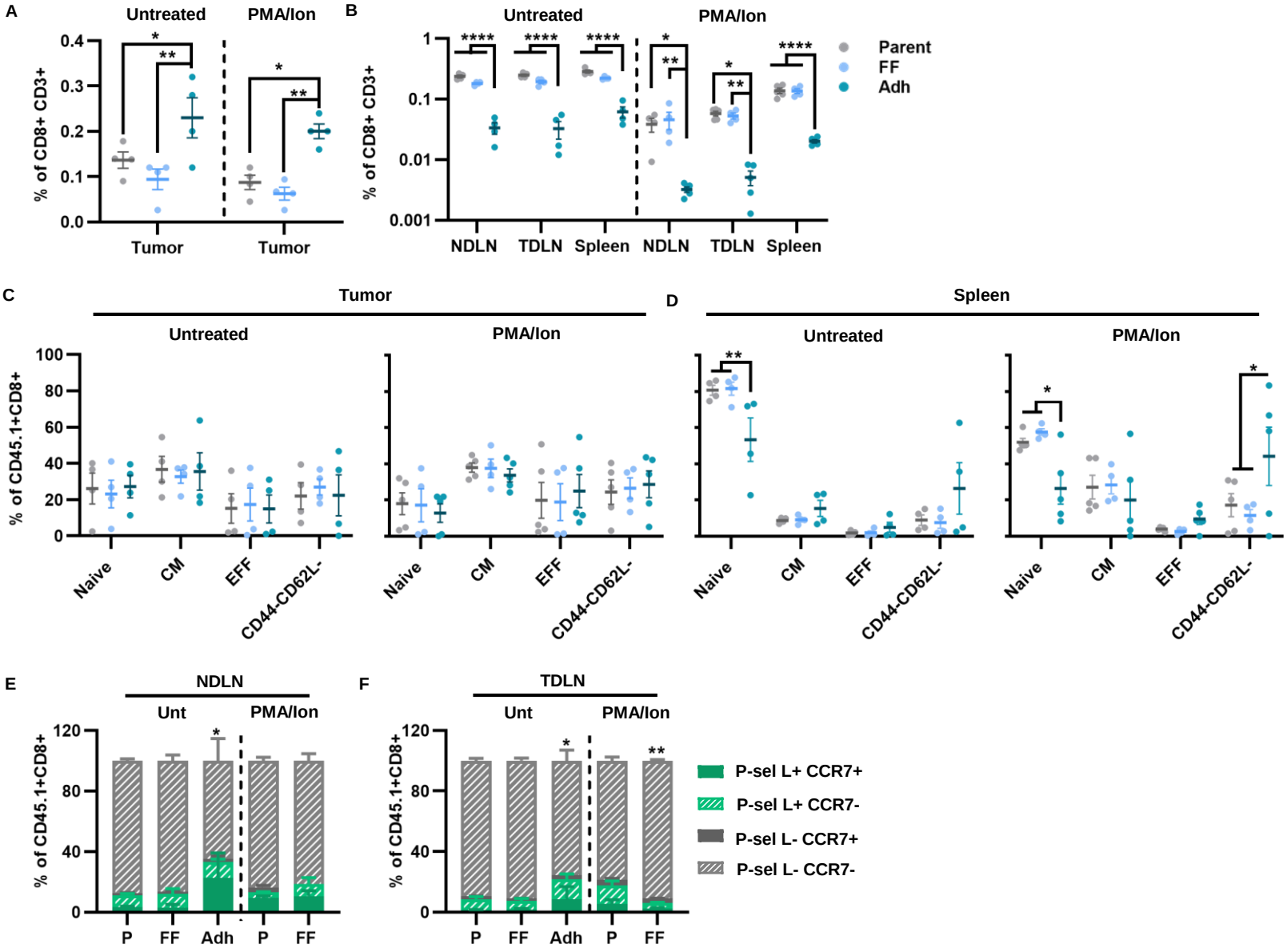

Supplemental Figure 10. CD8+ T-cell adherent fraction has enhanced tumor homing and reduced accumulation within lymphoid tissues compared to free flow fraction and unsorted population independent of donor cell pre-treatment. Related to Figure 4. A-B) Frequency of donor CD8+ T-cells of all CD8+ T-cells recovered from various tissues. C) Frequency of adoptively transferred untreated and PMA/Ion CD8+ T-cells recovered from the tumor of various subtypes. D) Frequency of adoptively transferred untreated and PMA/Ion CD8+ T-cells recovered from the spleen of various subtypes. E-F) Frequency of single- and co-expression of P-selectin ligand and CCR7 by donor CD8+ T-cells that were untreated or pretreated with PMA/Ion recovered from NDLN and TDLN 16 h post transfer. Each point represents one individual animal. Data represents mean ± s.e.m of 3 or more independently run experiments; two-way ANOVA with Tukey's multiple comparisons test; * $p<0.05$, ** $p<0.01$, **** $p<0.0001$.

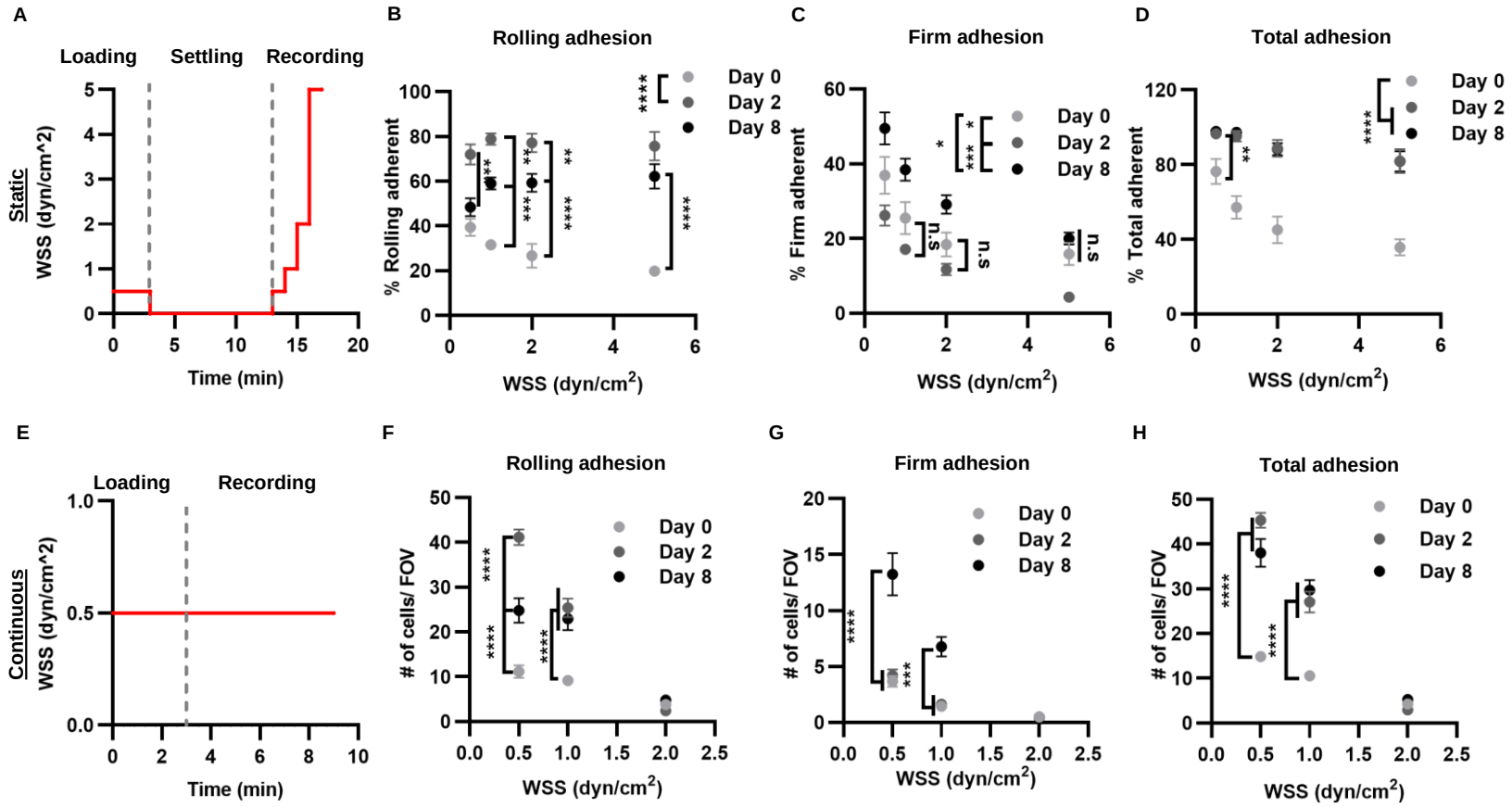

Supplemental Figure 11. CD8+ T-cells at different days of Dynabead and IL-2 expansion exhibit differential adhesive behaviors to P-selectin in physiological flow. Related to Figure 5. A) Schematic outlining perfusion workflow for static condition. Percent of rolling adhesion (B), firm adhesion (C), and total adherent cells (D) per field of view on P-selectin functionalized flow chamber under static perfusion conditions at various levels of wall shear stress at 0.5x10^6 cells/ml. E) Schematic outlining perfusion workflow for continuous flow. Number of rolling (F), firm (G), and total (H) interacting CD8+ T-cells per field view on P-selectin substrate under continuous flow condition at various levels of wall shear stress at 0.5x10^6 cells/ml. Data represents mean ± s.e.m of 3 or more independently run experiments; two-way ANOVA with Tukey's multiple comparisons test; * p<0.05, **p<0.01, *** p<0.001, ****p<0.0001. n.s., not significant.

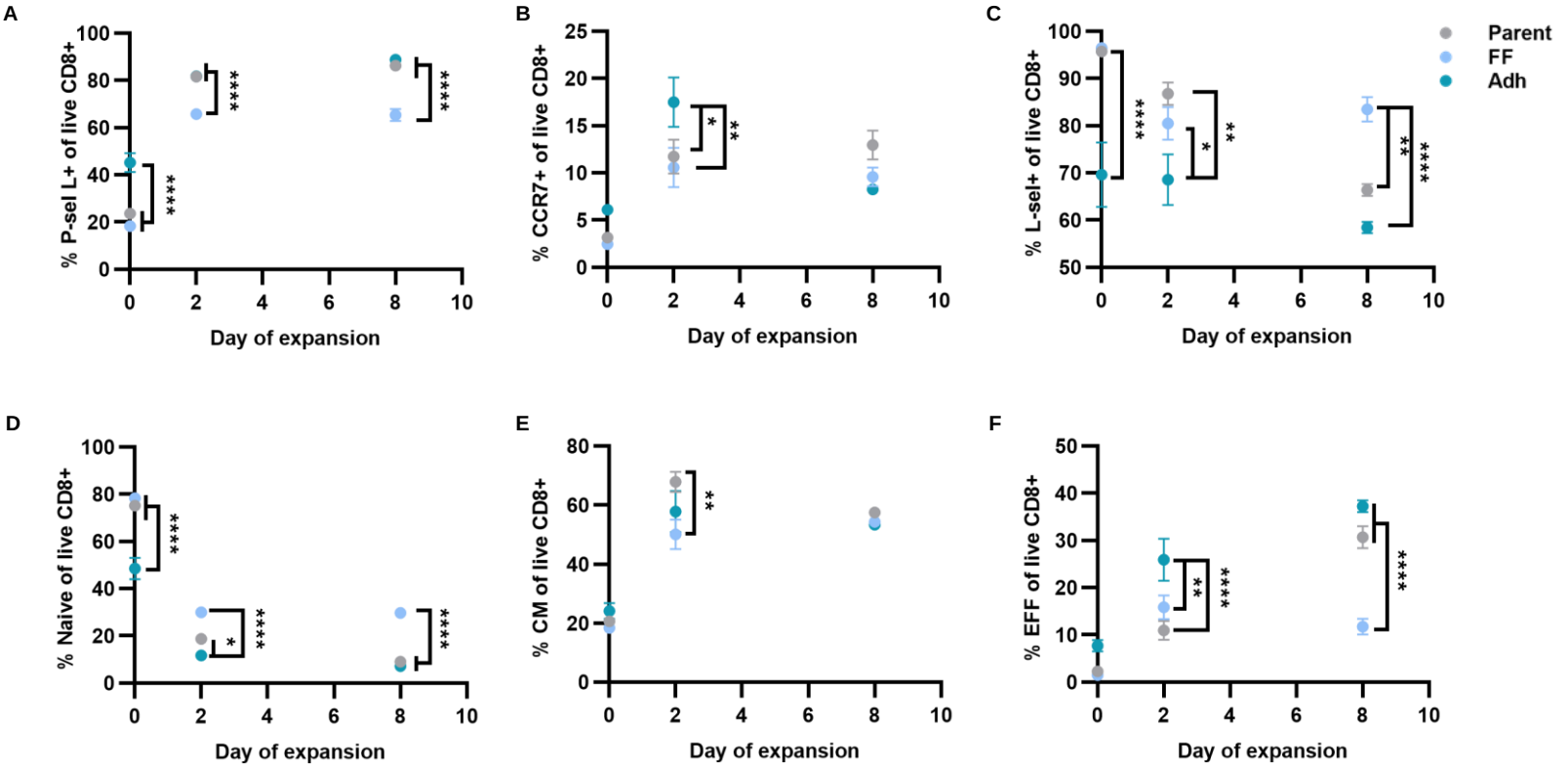

Supplemental Figure 12. Differential adhesive ligand expression by CD8+ T-cells at different days of expansion enriched for adhesion to P-selectin in flow using adhesion chromatography microfluidic system. Related to Figure 5. Frequency of P-selectin ligand (A), CCR7 (B) and L-selectin (C) expressing CD8+ T-cells and fraction of naïve (D), CM (E) and EFF (F) subtypes recovered from unsorted, free flow (FF), or adherent (Adh) fractions at different days of expansion. Data represents mean ± s.e.m of 3 or more independently run experiments; two-way ANOVA with Tukey's multiple comparisons test; * $p<0.05$, **$p<0.01$. *** $p<0.001$, ****$p<0.0001$.

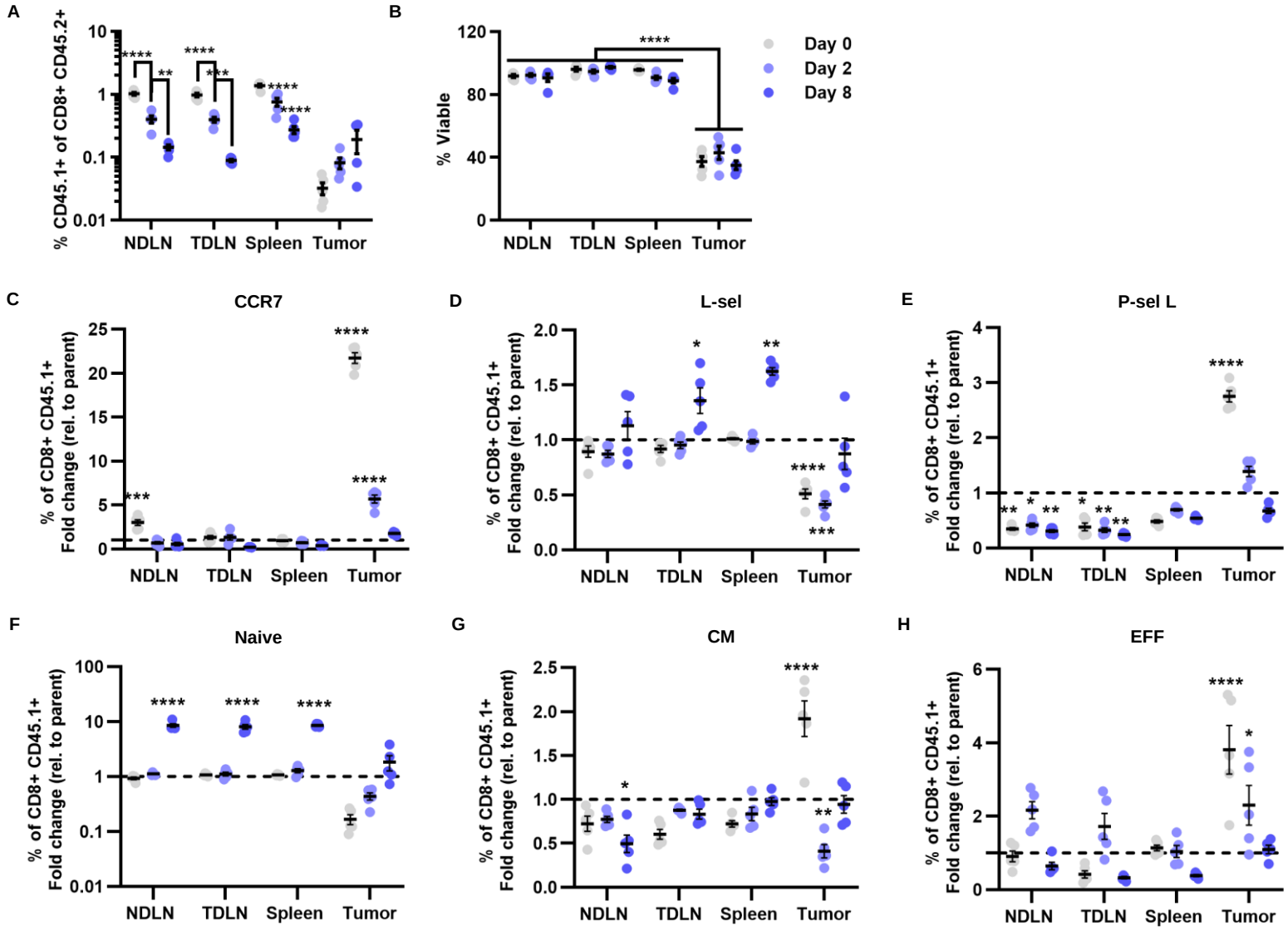

Supplement Figure 13. CD8+ T-cells exhibit differential *in vivo* homing capabilities depending on day of expansion. Related to Figure 5. A) Frequency of donor CD8+ T-cells (CD45.1+CD45.2-) of all CD8+ T-cells recovered from various tissues 16 h post transfer. B) Viability of recovered donor cells in each analyzed tissue. Fold change in the fraction of recovered donor (CD45.1+) CD8+ T-cells expressing CCR7 (C), L-selectin (D), and P-selectin ligand (E) and of a naïve (F), CM (G), and EFF (H) subtype within each tissue relative to their prevalence in the donor population pre-transfer. Each point represents results from an individual mouse. Data represents mean ± s.e.m of 3 or more independently run experiments. Statistical comparisons by two-way ANOVA with Tukey's multiple comparisons test. * p<0.05, **p<0.01, *** p<0.001, ****p<0.0001.

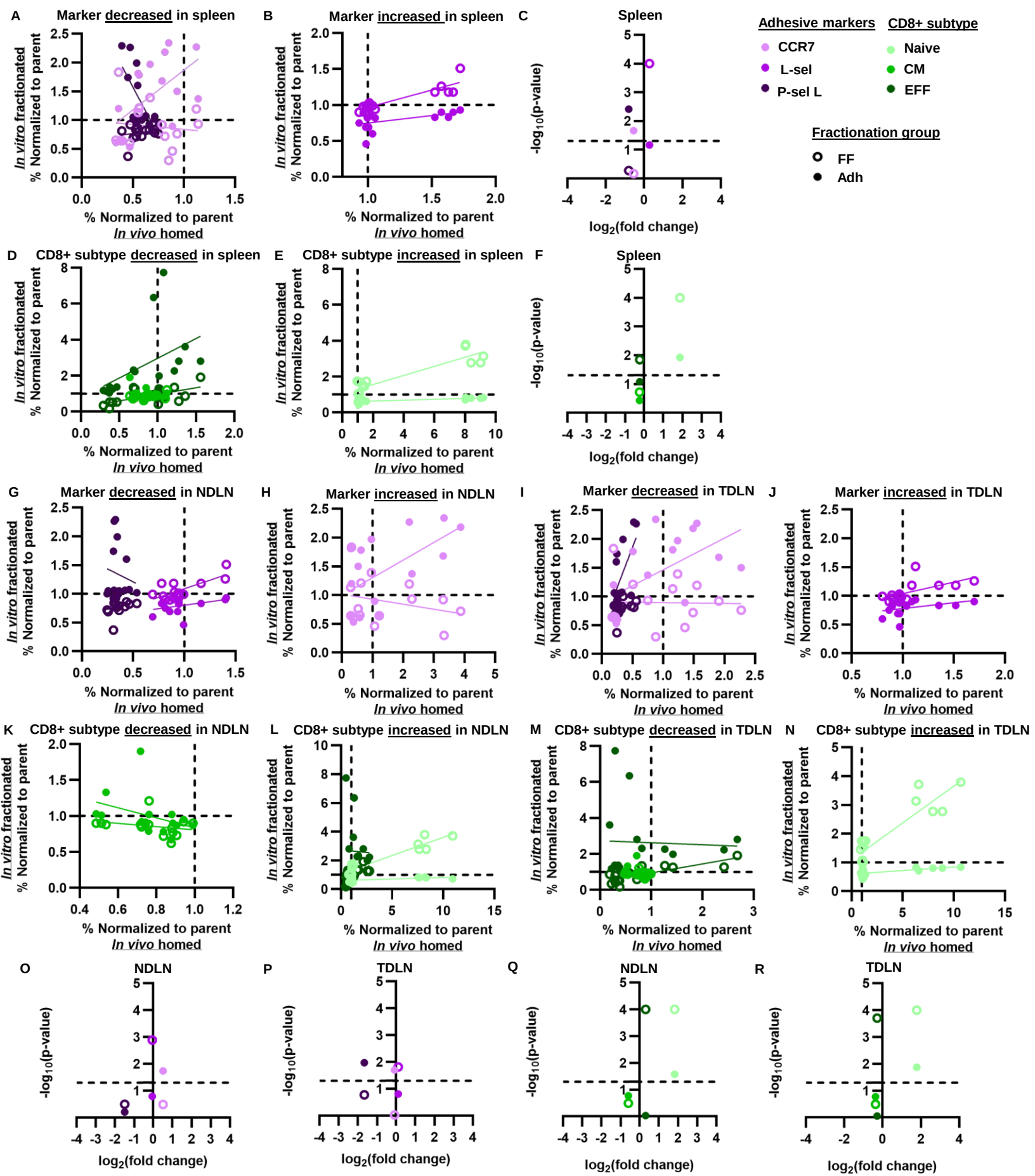

Supplemental Figure 14. Correlation analysis of CD8+ T-cells enriched based on *in vitro* adhesion vs. tissue-specific trafficking. Related to Figure 5. Correlation analysis of adhesion molecule expression (A-B, G-J) and subtype (D-E, K-N) enrichment between CD8+ T-cells enriched for adhesion to P-selectin in flow and that traffic to the spleen (A-B, D-E), NDLN (G-H, K-L) and TDLN (I-J, M-N) 16 h post transfer. $-\log_{10}$(p-value) versus $\log_2$(fold change) of adhesion molecule expression (C, O-P) and subtype (F, Q-R) by CD8+ T cells recovered from the spleen, NDLN, and TDLN.). A-B, D-E, G-N, each point represents results from an individual animal.

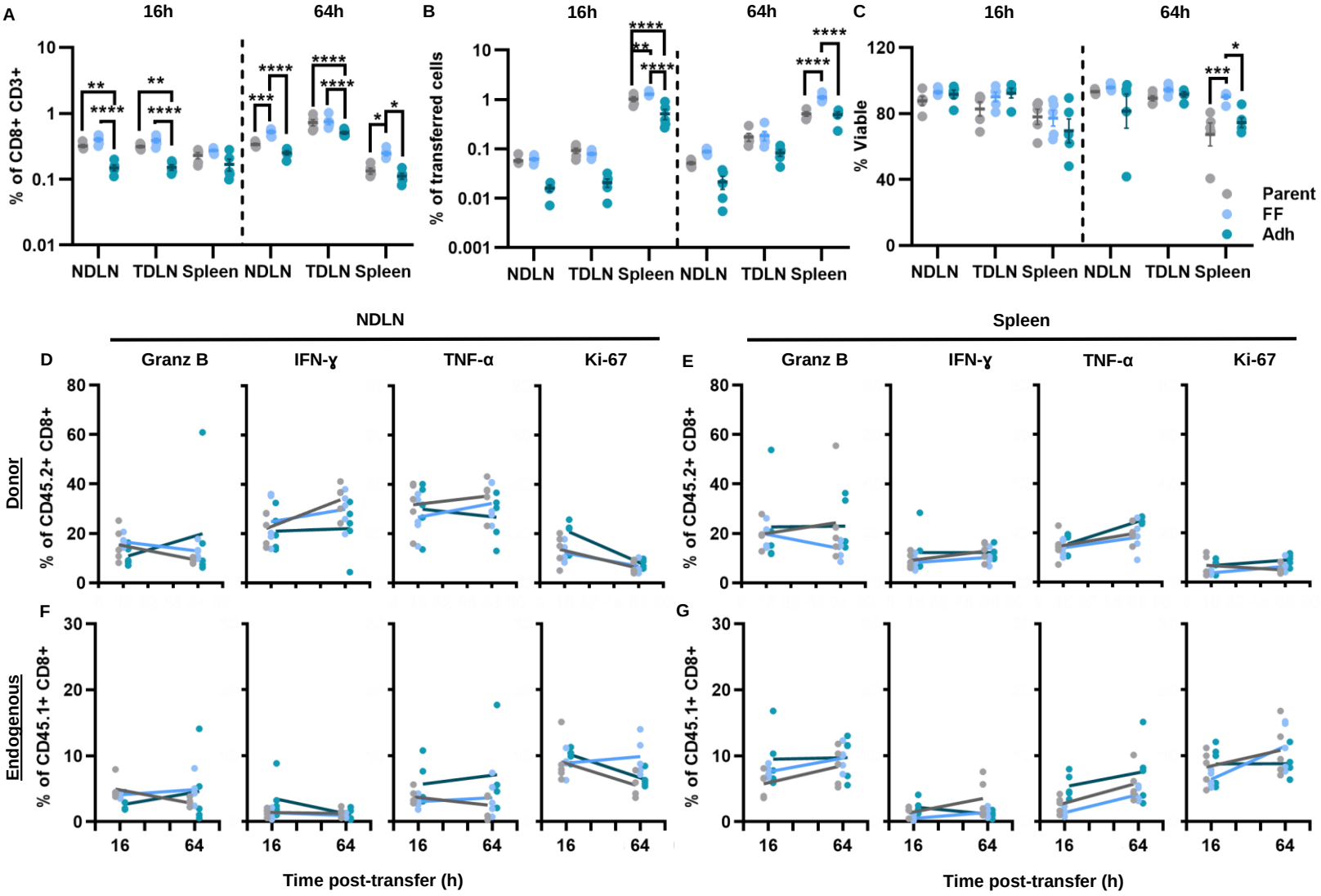

Supplemental Figure 15. OT-I CD8+ T-cells recovered in the adherent fraction have reduced trafficking into LNs. Related to Figure 6. A) Frequency of donor CD8+ T-cells recovered in various lymphoid tissues. B) Donor CD8+ T-cells recovered in various lymphoid tissues as a frequency of the total number of cells transferred into the B16F10-OVA tumor-bearing mice. C) Viability of donor CD8+ T-cells in various lymphoid tissues. Percent of cytokine-producing, PD-1+, Ki-67 of donor CD8+ T-cells in the NDLN (D) or spleen (E). Percent of cytokine-producing, PD-1+ or Ki-67 of endogenous CD8+ T-cells in the NDLN (F) or spleen (G). Graphs represent mean ± s.e.m, (n=5); statistics were performed by two-way ANOVA with Tukey's multiple comparison test. (D-G); * indicates significance of comparison to parent population, $ indicates significance of comparison between time points. * p<0.05, **p<0.01. *** p<0.001, ****p<0.0001.

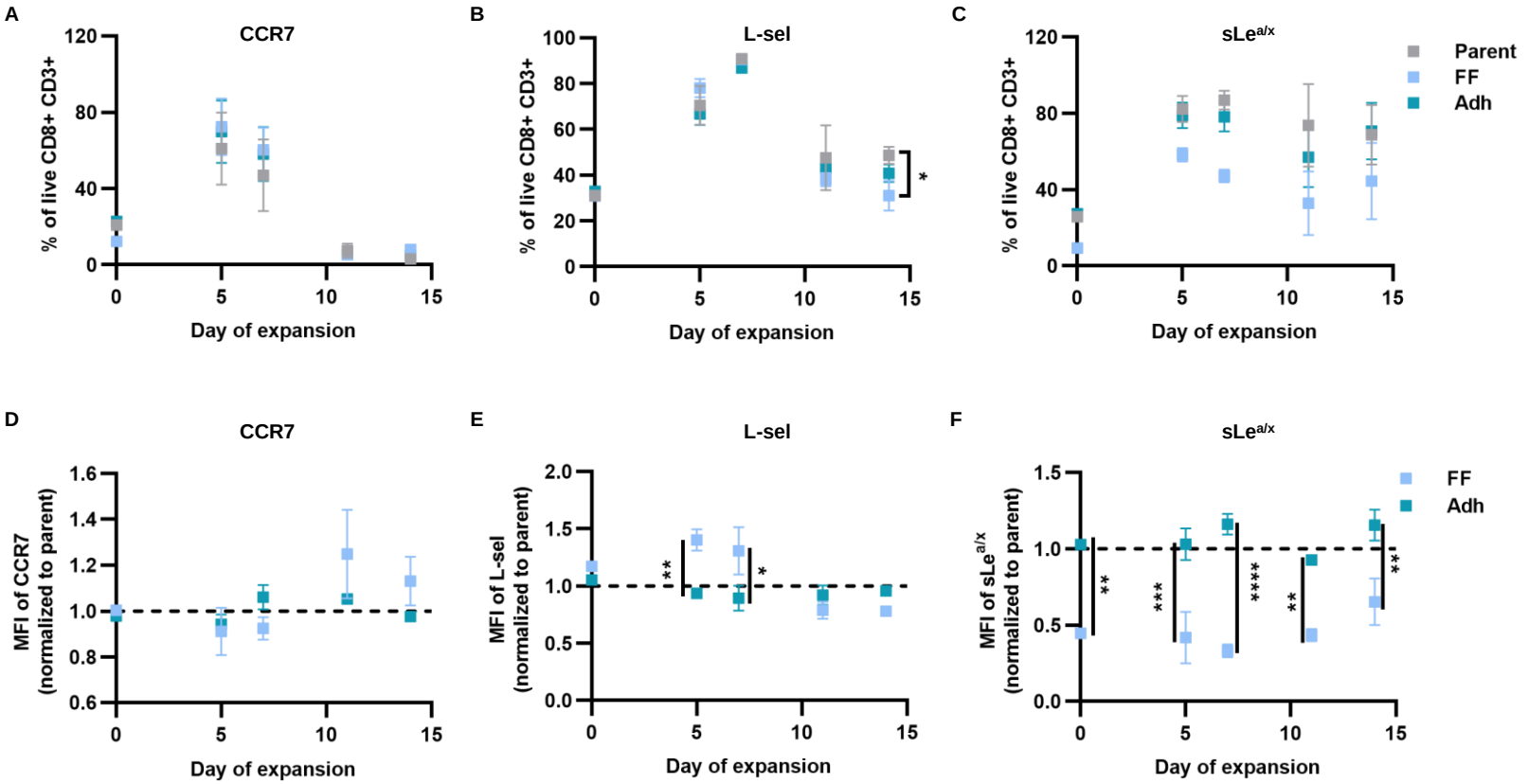

Supplemental Figure 16. Human CD8+ T-cells enriched for adhesion to P-selectin in physiological fluid flow exhibit different extents of adhesion molecule expression that varies by day of expansion. Related to Figure 7. Frequency (A-C) and fold change in MFI relative to parent population (D-F) of CCR7 (A, D), L-selectin (B, E), $sLe^{a/x}$ (C, F) adhesion molecules of live CD8+ T-cells at different days of expansion in parent or FF or Adh fractions recovered from P-selectin functionalized adhesion chromatography channel. Data represents mean ± s.e.m of 3 or more independently run experiments; two-way ANOVA with Bonferroni's multiple comparisons test; * p<0.05, **p<0.01. *** p<0.001, ****p<0.0001.